

## Preparation of Isothermally Crystallized $\gamma$ -Form Poly(vinylidene fluoride) Films by Adding a KBr Powder as a Nucleating Agent

Tsukasa Miyazaki,\* Yuuki Takeda, Midori Akasaka, Miki Sakai, and Akie Hoshiko

Core Technology Center, Nitto Denko Corporation, 1-1-2, Shimohozumi, Ibaraki, Osaka 567-8680, Japan

Received December 4, 2007

Revised Manuscript Received January 21, 2008

### Introduction

Poly(vinylidene fluoride) (PVDF) has been widely studied for the purpose of various applications such as piezoelectric and pyroelectric materials.<sup>1</sup> It is well-known that PVDF exhibits many crystalline modifications. The  $\alpha$ -form is predominantly obtained during crystallization from the melt. The  $\beta$ -form, which consists of planar zigzag conformation, has been most widely attractive for the electric properties. The  $\beta$ -form has been shown to be obtained with casting methods using selective solvents such as *N,N*-dimethylacetamide (DMAc) and *N,N*-dimethylformamide<sup>2–5</sup> or with mechanical stretching methods of the  $\alpha$ -form films at a relatively low draw temperature.<sup>6,7</sup>

The third polymorph is the so-called  $\gamma$ -form, which is generally obtained with isothermal crystallization from the melt at a relatively high crystallization temperature or annealing at a high temperature<sup>8–12</sup> as well as with the solution casting methods with selective solvents.<sup>2</sup> Two types of  $\gamma$ -form crystallites are produced in the film during isothermal crystallization at a relatively high temperature. One of these is the  $\gamma$ -form crystallites originated from the nucleating and growth with a low growth rate ( $\gamma$ -crystallites) in the coexisting  $\alpha$ -form crystallites with a high growth rate. Other  $\gamma$ -form crystallites are produced with the solid–solid phase transition from the already grown  $\alpha$ -form crystallites to the  $\gamma$ -form ones ( $\gamma'$ -crystallites).<sup>8–12</sup>

The development of these two types of  $\gamma$ -form crystallites was fully investigated with many researchers, such as Prest et al.,<sup>8,9</sup> Osaki et al.,<sup>10</sup> and Lovinger.<sup>11,12</sup> Osaki et al. indicated that a PVDF film with a large amount of the  $\gamma$ -form crystallites ( $\gamma$ -form-rich film) was obtained after isothermal crystallization at 165–175 °C for at least 20 h. Prest et al. also found that the sample after isothermal crystallization at 158 °C for 15 h consists of 40.5%  $\alpha$ -form crystallites and 7.2%  $\gamma$ -form ones, but after isothermal crystallization at the same temperature for 95 h, the sample contains 11.2%  $\alpha$ -form crystallites and 34.8%  $\gamma$ -form ones. The detail morphological investigation was performed by Lovinger,<sup>11,12</sup> indicating that the growth rate of the  $\gamma$ -crystallites is reduced to be 3 times lower than that of the  $\alpha$ -form ones and that the consequent large  $\alpha$ -form spherulites are transformed into the  $\gamma$ -form ones at 155–162 °C for 3 days.

These pioneering works suggested that at a high crystallization temperature the growth rate of the  $\gamma$ -crystallites is very low compared to that of the  $\alpha$ -form ones, and the phase transition of the  $\alpha$ -form crystallites to the  $\gamma'$ -crystallites proceeds very slowly. Therefore, it is difficult to obtain a  $\gamma$ -form-rich film with isothermal crystallization and to observe the process of

the solid–solid phase transition of the  $\alpha$ -form crystallites to the  $\gamma$ -form ones by a time-resolved characterization method in order to investigate the transition behavior in detail.

In this Note, it will be described that a  $\gamma$ -form-rich PVDF film isothermally crystallized is easily obtained by adding a KBr powder as a nucleating agent to the polymer–solvent system. First of all, Lovinger found that PVDF crystallites epitaxially grow on KBr, NaCl, and mica surfaces.<sup>13–15</sup> Therefore, it is expected that these materials act as a nucleating agent for PVDF. We demonstrate that for the PVDF film containing KBr particles the  $\gamma$ -form crystallites are predominantly produced during isothermal crystallization at a relatively high temperature for a short time. This simple preparation method of a  $\gamma$ -form rich film may also contribute to the detail investigation of the transition mechanism of the  $\alpha$ -form crystallites to the  $\gamma$ -form ones.

### Experimental Section

The PVDF resin made by Kureha Co. (KF polymer) with the weight-average molecular weight of about 250 000 were used in this study. Samples of various thicknesses were prepared for different measurements using the solution casting method. The neat PVDF films and the PVDF films containing a nucleating agent were prepared from *N*-methyl-2-pyrrolidone and DMAc solutions, respectively. Three kinds of nucleating agents were examined in this study. One of these is a KBr powder (Aldrich Chemical Co.). Other nucleating agents are talc (Kanto Kagaku Co.) and sodium 2,2'-methylenbis(4,6-di-*tert*-butylphenylene)phosphate (NA11; ADEKA Co.), which are usually used as an additive to polyethylene and polypropylene.<sup>16,17</sup> The KBr powder was further ground with a mortar for 2 h before using because it does not have a fine particle size suitable to use as a nucleating agent. NA11 and talc used in this study are commercially supplied as a nucleating agent. Therefore, NA11 and talc were used as received.

PVDF compounds were dissolved in DMAc solution. Initial solution concentration was 10 wt %. The solution was filtered (6  $\mu$ m pore size) for removing dust, followed by adding a nucleating agent of 0.1, 1, or 5 wt % of the polymer. The solution was fully stirred prior to casting. Then, the solution was cast on a cleaned glass plate and dried in an air oven.

Differential scanning calorimetry (DSC) measurements were performed using a Diamond DSC (Perkin-Elmer Co.) equipped with an intracooler 2P cooling accessory. The temperature and heat flow at difference heating rates were calibrated using an indium and tin standard with nitrogen purging. The PVDF samples, which are cut from a casting film with a thickness of about 50  $\mu$ m, were weighed and sealed in an aluminum pan. Then the samples were melted at 250 °C for 5 min to erase previous thermal history. In the isothermal crystallization experiment, the samples were quenched to various desired temperatures at a cooling rate of about 150 °C/min. The reference material was an empty pan.

The Fourier transform infrared spectroscopy (FT-IR) measurements of the films during isothermal crystallization were performed on a Varian 3100 FT-IR spectroscope (Varian Co.) equipped with a temperature-controlled cell (Linkam THMS 600, Japan Hitech Co.). In the measurements using the temperature-controlled cell, the cooling rate is about 300 °C/min. The selection of the window material is a crucial issue in testing the nucleating agent effects on isothermal crystallization of polymer matrixes containing an additive without any interfacial effects, such as transcrystallization on a window material.<sup>18</sup> Benkhati et al. reported that for PVDF samples transcrystallization is observed on various substrates, but it does not develop on glass and aluminum substrates.<sup>19</sup> Therefore, in this FT-IR study, Si wafers with a native oxide layer were used as

\* To whom correspondence should be addressed: e-mail tsukasa\_miyazaki@g.nitto.co.jp, Ph +81-72-621-0265, Fax +81-72-621-0316.

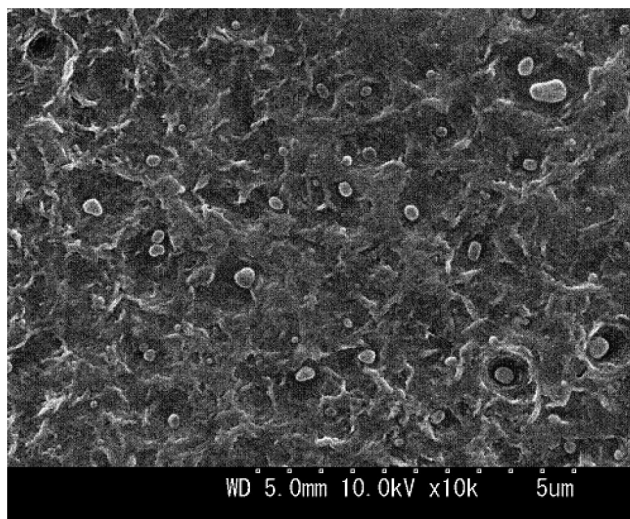


**Figure 1.** Scanning electron microscopic image of the surface of the PVDF film containing 1 wt % KBr.

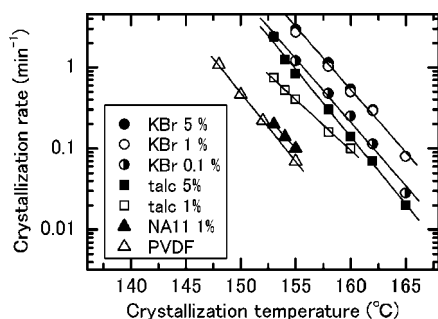


**Figure 2.** Crystallization rate derived from the inversion of the exothermic peak time during isothermal crystallization using DSC for the PVDF films containing nucleating agents with various concentrations indicated in the figure. The solid lines are drawn to guide the eye.

windows because it is expected that this surface native oxide layer does not have any interfacial effects on isothermal crystallization of the PVDF film as well as glass substrates. In fact, in the observation of isothermal crystallization kinetics of the PVDF films using FT-IR, the crystallization rate substantially increases on usually used window materials, such as KBr and KCl compared to that on the Si wafer. This must be due to the transcristallization or epitaxial growth effects of these materials, as described below. It should be also noted that aluminum pans used in DSC measurements have not any interfacial effects on PVDF isothermal crystallization. The PVDF thin films of about 10–20  $\mu\text{m}$  thickness were sandwiched between two Si wafers for the measurements of FT-IR spectra during isothermal crystallization.

## Results and Discussion

The surface morphological image of the PVDF film with 1 wt % KBr was observed with scanning electron microscopy (Figure 1). KBr particles with a size of 0.2–0.3  $\mu\text{m}$  are uniformly dispersed in the polymer matrix. This figure indicates that the KBr powder purchased for this study should be fully ground for at least 2 h before adding to polymer–solvent systems as a nucleating agent.

The crystallization rates are derived from the DSC exothermic curves during isothermal crystallization at various temperatures, as shown in Figure 2. The crystallization rate is defined with the inversion of the exothermic peak time. It was found that KBr has superior nucleating ability compared to other two additives. The crystallization rate for the PVDF film with 1 wt

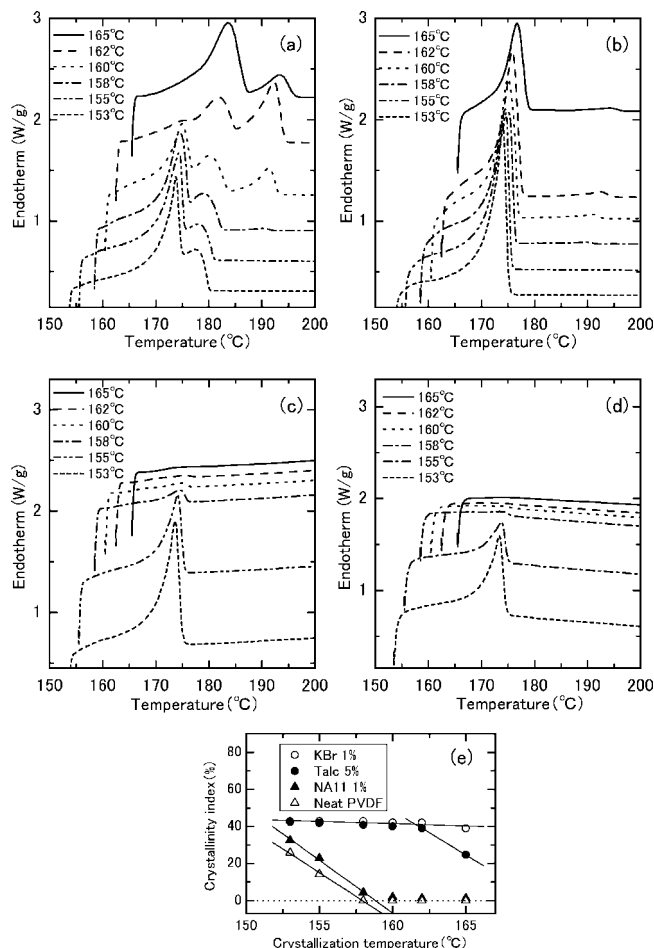


**Figure 3.** DSC endothermic curves for the PVDF films containing 1 wt % KBr (a), 5 wt % talc (b), 1 wt % NA11 (c), and the neat PVDF film (d) after isothermal crystallization at various temperatures. Each isothermal crystallization was performed at 153  $^{\circ}\text{C}$  for 10 min, 155  $^{\circ}\text{C}$  for 15 min, 158  $^{\circ}\text{C}$  for 20 min, 160  $^{\circ}\text{C}$  for 30 min, 162  $^{\circ}\text{C}$  for 50 min, and 165  $^{\circ}\text{C}$  for 100 min. Each data is vertically shifted for clarity. Part e shows the crystallinity indexes estimated with the endothermic peak areas for the films isothermally crystallized at each temperature. The solid lines in (e) are drawn to guide the eye.

% KBr is nearly equal to that for the PVDF film containing 5 wt % KBr at each temperature, indicating that KBr particles are effectively dispersed in the polymer matrix. Talc has also superior nucleating ability because the crystallization rates of the PVDF film containing 5 wt % talc are 10 times larger than those of the neat PVDF at each crystallization temperature, as shown in Figure 2.<sup>20–23</sup> The addition of NA11 does not almost affect the crystallization kinetics of the PVDF film, as shown in Figure 2.

Parts a–d of Figure 3 show the endothermic curves of the PVDF films containing 1 wt % KBr, 5 wt % talc, 1 wt % NA11, and the neat PVDF film after isothermal crystallization at various temperatures, respectively. The heating rate is 10  $^{\circ}\text{C}/\text{min}$ . Each isothermal crystallization was performed at 153  $^{\circ}\text{C}$  for 10 min, 155  $^{\circ}\text{C}$  for 15 min, 158  $^{\circ}\text{C}$  for 20 min, 160  $^{\circ}\text{C}$  for 30 min, 162  $^{\circ}\text{C}$  for 50 min, and 165  $^{\circ}\text{C}$  for 100 min. These times are confirmed to be fully long for the completion of crystallization of the PVDF film with 1 wt % KBr at each temperature. The neat PVDF and the PVDF containing NA11 do not almost crystallize in the examined time scale at a high temperature, as shown in Figure 3c,d. Figure 3e shows the crystallinity indexes estimated with the endothermic peak areas for the films after isothermal crystallization at each temperature. Here, the melting

heat enthalpy for each crystallite with different melting temperatures is assumed to be equal to that of the  $\alpha$ -form crystallite, 102.5 J/g.<sup>24</sup> Under this assumption, these crystallinity indexes can be only used to compare samples within this experiment for qualitative trends, and it should be noted that the value of the crystallinity index estimated differs from the absolute crystallinity index. Figure 3e also indicates that KBr has superior nucleating ability compared to other conventional additives. The PVDF film with 5 wt % talc is fully crystallized at each crystallization temperature except at 165 °C, implying that talc has also superior nucleating ability for PVDF.

There are three peaks in the endothermic curves for the PVDF film containing 1 wt % KBr isothermally crystallized above 158 °C, indicating that three kinds of crystallites having different polymorphs and/or sizes and/or perfections coexist in a film crystallized at a relatively high temperature, or melting and recrystallization take place in the heating scan.<sup>25–28</sup> In the case of the multiendothermic peaks of PVDF crystallized or annealed at a relatively high temperature, each endothermic peak has been confidently assigned by many researchers. That is to say, the lowest endothermic peak is attributed to the melting of the  $\alpha$ -form crystallites. The middle endothermic peak is considered to be due to the melting of the  $\gamma$ -crystallites, which are originated from the nucleating and growth in the polymer matrix, and the highest one is attributed to the melting of the  $\gamma'$ -crystallites, which are produced with the phase transition of the  $\alpha$ -form crystallites to the  $\gamma$ -form ones.<sup>29–31</sup> For the PVDF film with 1 wt % KBr, the middle endothermic peak can be observed in the endothermic curve even for the sample isothermally crystallized at 153 °C, as shown in Figure 3a. On the other hand, the middle endothermic peak does not appear in all endothermic curves for the PVDF film containing 5 wt % talc, although a small amount of the  $\gamma'$ -crystallites seems to exist in the film isothermally crystallized above 158 °C. It is well-known that at a relatively low crystallization temperature, such as 153 °C, the  $\alpha$ -form crystallites predominantly grow, and the  $\gamma$ -crystallites cannot exist owing to a substantial low growth rate compared to that of the  $\alpha$ -form crystallites.

Furthermore, the middle endothermic peak area increases with isothermal crystallization temperature compared to the sum of other two peak areas, implying that KBr increases relatively the crystallization rate of the  $\gamma$ -crystallites to that of the  $\alpha$ -form ones with increasing the crystallization temperature. On the other hand, talc increases only the crystallization rate of the  $\alpha$ -form crystallites and may not affect the crystallization rate of the  $\gamma$ -crystallites. Moreover, for the PVDF film containing 1 wt % KBr the relative peak area of the highest endothermic peak to that of the lowest one increases with isothermal crystallization temperature. On the other hand, in the case of the PVDF film containing 5 wt % talc, the peak area of the highest endothermic peak does not increase relatively to that of the lowest one, indicating that the solid–solid phase transition of the  $\alpha$ -form crystallites to the  $\gamma$ -form ones is accelerated in the case of the PVDF film containing 1 wt % KBr compared to that of the PVDF film with 5 wt % talc. Consequently, the PVDF film containing 1 wt % KBr after isothermal crystallization at 165 °C is a  $\gamma$ -form-rich film, as shown in Figure 3a.

For the PVDF film containing 1 wt % KBr and that with 5 wt % talc, wide-angle X-ray diffraction measurements were performed using Cu K $\alpha$  radiation. Figure 4a shows the X-ray diffraction results for the PVDF film with 1 wt % KBr and that with 5 wt % talc isothermally crystallized at 165 °C. The crystallization times are 100 and 250 min for the PVDF film with 1 wt % KBr and that with 5 wt % talc, respectively. It

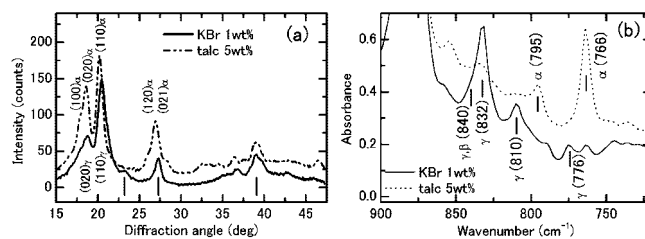


**Figure 4.** (a) Wide-angle X-ray diffraction profiles of the PVDF film containing 1 wt % KBr and 5 wt % talc isothermally crystallized at 165 °C. The crystallization times are 100 and 250 min for the PVDF film with 1 wt % KBr and that with 5 wt % talc, respectively. The vertical lines indicate the diffraction peak positions from the KBr particles in the film with 1 wt % KBr. Part b indicates the IR spectra of the PVDF film containing 1 wt % KBr and that with 5 wt % talc after isothermal crystallization at 165 °C for 100 and 250 min, respectively. Each data in the figure is vertically shifted for clarity.

was found that the diffractogram of the PVDF film containing 5 wt % talc is identical to that originated from the  $\alpha$ -form crystallites. On the other hand, the diffractogram of the PVDF film with 1 wt % KBr should be originated from the  $\gamma$ -form crystallites, although a small amount of the  $\alpha$ -form and/or  $\beta$ -form ones may be contained in the film. These results seem to confirm the assignment of the DSC multiendothermic peaks shown in Figure 3a,b. However, in the diffractogram of the PVDF film with 1 wt % KBr the strong diffraction peaks originating from the KBr particles, which are shown by the vertical lines in Figure 4a, are overlapped with those originating from the PVDF crystallites. Therefore, using IR spectra, it should be exactly confirmed whether the PVDF film containing 1 wt % KBr is  $\gamma$ -form-rich or not after isothermal crystallization at 165 °C.

Figure 4b shows the IR spectra for the PVDF film containing 1 wt % KBr and that with 5 wt % talc after isothermal crystallization at 165 °C for 100 and 250 min, respectively. This figure elucidates that the PVDF film containing 1 wt % KBr is a  $\gamma$ -form-rich film rather than an  $\alpha$ -form one after isothermal crystallization at 165 °C because of the existence of the absorption band of 810 and 776 cm<sup>-1</sup>, which are exclusively associated with the  $\gamma$ -form crystallites,<sup>2,9,32</sup> and the absence of the 795 and 766 cm<sup>-1</sup>, which are exclusively characteristic to the  $\alpha$ -form ones,<sup>2,9,32</sup> although a tiny 766 cm<sup>-1</sup> band intensity can be observed in the spectrum. Furthermore, the absorption band of 832 cm<sup>-1</sup> characteristic of the  $\gamma$ -form crystallites can be distinguished from the 840 cm<sup>-1</sup> band, which is considered to be common to both crystallites of the  $\gamma$ -form and the  $\beta$ -form, implying that the PVDF film with KBr exclusively contains the  $\gamma$ -form crystallites rather than the  $\beta$ -form ones, as suggested by Gregorio.<sup>32</sup> On the other hand, in the case of the PVDF film with 5 wt % talc after isothermal crystallization at 165 °C, only the absorption bands of 766 and 795 cm<sup>-1</sup> are observed in the film, as shown in Figure 4b. These results confirm that the PVDF films containing 1 wt % KBr is  $\gamma$ -form-rich after isothermal crystallization at 165 °C, although a small amount of the  $\alpha$ -form and/or  $\beta$ -form crystallites may be included in the film. On the other hand, it is concluded that the PVDF film with 5 wt % talc is  $\alpha$ -form rich after isothermal crystallization at 165 °C.

Figure 5a,b shows the endothermic curves for the samples containing 1 wt % KBr and 5 wt % talc after isothermal crystallization at 165 °C for various times. Figure 5c shows the crystallinity index derived from the endothermic peak area in each endothermic curve, such as that described in Figure 3e. The figure indicates that the increases in the crystallinity index for the films containing 1 wt % KBr and 5 wt % talc level off



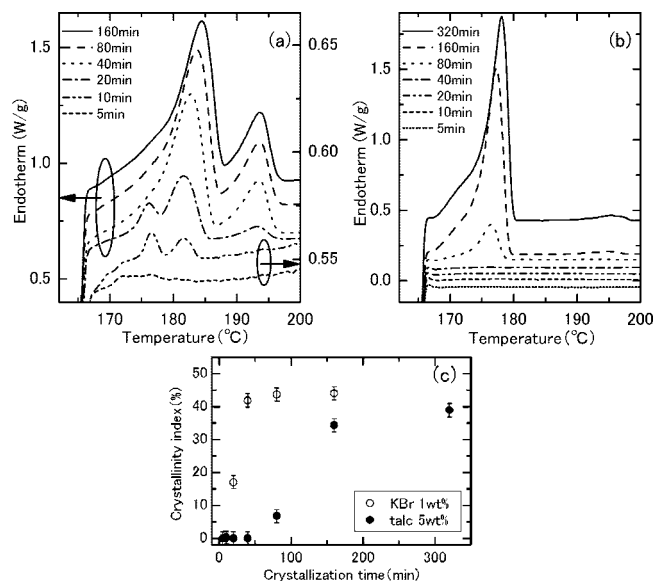


**Figure 5.** DSC endothermic curves for the PVDF films containing 1 wt % KBr (a) and 5 wt % talc (b) isothermally crystallized at 165 °C for various times indicated in the figure. Each data in (a) and (b) is vertically shifted for clarity. Part c shows the crystallinity index derived from the endothermic peak area in each endothermic curve.

above 40 and 150 min, respectively. As shown in Figure 5a, in the case of the PVDF film with 1 wt % KBr, the middle endothermic peak substantially increases with time, and the relative endothermic peak area of the highest endothermic peak to that of the lowest one increases with time. However, for the PVDF film containing 5 wt % talc the middle endothermic peak is not observed even after isothermal crystallization for 320 min, and the relative peak area of the highest endothermic peak to that of the lowest one is kept at a low level, also implying that KBr promotes relatively the crystallization rate of the  $\gamma$ -crystallites to that of the  $\alpha$ -form ones, and the solid–solid phase transition of the  $\alpha$ -form crystallites to the  $\gamma$ -form ones at a high temperature compared to the case of the neat PVDF or PVDF with other additives. After isothermal crystallization at 165 °C for 900 min, a substantial increase in the highest endothermic peak area can be observed for the PVDF film containing 5% talc as well as the neat PVDF film. However, the middle endothermic peak does not appear even in that case, also indicating that talc particles increase only the crystallization rate of the  $\alpha$ -form crystallites.

In the crystallization time of 10–20 min, for the PVDF film containing 1 wt % KBr, the  $\alpha$ -form crystallites and the  $\gamma$ -crystallites coexist in the sample, as shown in Figure 5a, indicating that the crystallization rates of two types of crystallites are comparable in the early time of crystallization. However, the amount of the  $\alpha$ -form crystallites decreases above the crystallization time of 20 min, and on the contrary the amount of the  $\gamma$ -crystallites increases after the crystallization time of 20 min. This should be an evidence of the solid–solid phase transition of the  $\alpha$ -form crystallites to the  $\gamma$ -form ones. However, this may be due to melting and recrystallization on heating.

For obtaining a direct evidence of the phase transition, we observed the FT-IR spectra during isothermal crystallization at 165 °C for the PVDF film containing 1 wt % KBr and the PVDF film containing 5 wt % talc. The development of the peak intensities of 766 and 810  $\text{cm}^{-1}$ , which are assigned to be the absorption band of the  $\alpha$ -form crystallites and that of the  $\gamma$ -form ones, respectively, was examined with crystallization time. In the Figure 6a,b, the differential peak intensities from the

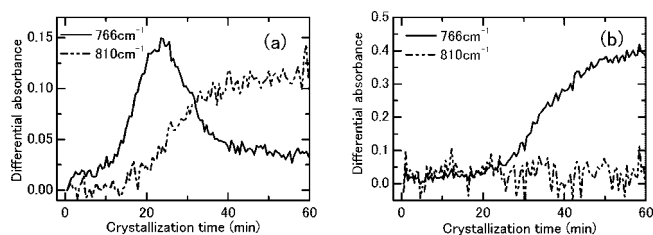


**Figure 6.** Development of the 766 and 810  $\text{cm}^{-1}$  absorption band intensities in FT-IR spectra obtained during isothermal crystallization at 165 °C for the PVDF film containing 1 wt % KBr (a) and the PVDF film containing 5 wt % talc (b).

spectrum obtained at the crystallization time of 0 min are plotted with time. It was found that both band intensities of 766 and 810  $\text{cm}^{-1}$  increase in the early time of crystallization for the PVDF film containing 1 wt % KBr, also indicating that the  $\alpha$ -form crystallites and the  $\gamma$ -crystallites coexist and the crystallization rates of the two types of crystallites are comparable in the early time of crystallization at 165 °C. However, the peak intensity of 766  $\text{cm}^{-1}$  assigned to be the absorption band of the  $\alpha$ -form crystallites rapidly decreases above 20 min, implying that the phase transition of the  $\alpha$ -form crystallites to the  $\gamma$ -form ones occurs predominantly above 20 min. Eventually, the  $\gamma$ -form crystallites dominantly exist in the film after isothermal crystallization for about 40 min, as shown in Figure 6a. These results obtained are good agreement with the DSC measurements results, as shown in Figure 5a,c. On the other hand, in the case of the PVDF film containing 5 wt % talc only the 766  $\text{cm}^{-1}$  band intensity monotonically increases with time, and the 810  $\text{cm}^{-1}$  band intensity does not quite increase in the examined time scale, implying that the  $\gamma$ -crystallites are not produced and the solid–solid phase transition of the  $\alpha$ -form crystallites to the  $\gamma$ -form ones does not occur in the examined time scale.

It is concluded that in isothermal crystallization at a high temperature KBr particles act as a nucleating agent for the  $\gamma$ -form crystallites rather than the  $\alpha$ -form ones and accelerate the solid–solid phase transition of the  $\alpha$ -form crystallites to the  $\gamma$ -form ones. On the other hand, talc particles promote only the crystallization rate of the  $\alpha$ -form crystallites and may not affect that of the  $\gamma$ -crystallites. Consequently, we found that a PVDF film with a large amount of the  $\gamma$ -form crystallites can be obtained with isothermal crystallization at 165 °C for about 40 min by adding a KBr powder as a nucleating agent, although in the case of PVDF films without nucleating agents, it is difficult to obtain a  $\gamma$ -form-rich film, even after isothermal crystallization for 100 h at the same temperature.<sup>8–12</sup> This must be attributed to the epitaxial growth of the  $\gamma$ -form PVDF crystallites on KBr surfaces originally described by Lovinger,<sup>13</sup> although he stated that on the KBr surface the  $\beta$ -form crystallites preferentially grow. This previous work was performed under slightly different conditions and with a different PVDF grade. These may explain the observed differences. Otherwise, at a relatively high temperature such as that examined in this study, the  $\gamma$ -form crystallites may preferentially grow in the PVDF film containing KBr particles, except in the interfacial regions between the polymer matrix and the KBr surface investigated by Lovinger, because the  $\gamma$ -form crystallites are much stable than the  $\beta$ -form ones at a high temperature. The preferential growth mechanism of PVDF crystallites in the film and the surface regions of the KBr particles should be further investigated, including the solid–solid phase transition of the  $\alpha$ -form crystallites to the  $\gamma$ -form ones.

## References and Notes

- (1) Nalwa, H. S., Ed. *Ferroelectric Polymers*; Marcel Dekker: New York, 1995.
- (2) Kobayashi, M.; Tashiro, K.; Tadokoro, H. *Macromolecules* **1975**, *8*, 158.
- (3) Weinhold, S.; Litt, M. H.; Lando, J. B. *J. Polym. Sci., Polym. Lett.* **1979**, *17*, 585.
- (4) Gregorio, R.; Cestari, M. *J. Polym. Sci., Part B: Polym. Phys.* **1994**, *32*, 859.
- (5) Salimi, A.; Tousefi, A. A. *J. Polym. Sci., Part B: Polym. Phys.* **2004**, *42*, 3487.
- (6) Lando, J. B.; Olf, H. G.; Peterlin, A. J. *J. Polym. Sci., Part A-1* **1966**, *4*, 941.
- (7) Matsushige, K.; Nagata, K.; Imada, S.; Takamura, T. *Polymer* **1980**, *21*, 1391.
- (8) Prest, W. M.; Luca, D. J. *J. Appl. Phys.* **1975**, *46*, 4136.
- (9) Prest, W. M.; Luca, D. J. *J. Appl. Phys.* **1978**, *49*, 5042.
- (10) Osaki, S.; Ishida, Y. *J. Polym. Sci., Part B: Polym. Phys.* **1975**, *13*, 1071.
- (11) Lovinger, A. J. *Polymer* **1980**, *21*, 1317.
- (12) Lovinger, A. J. *J. Polym. Sci., Part B: Polym. Phys.* **1980**, *18*, 793.
- (13) Lovinger, A. J. *Polymer* **1981**, *22*, 412.
- (14) Lovinger, A. J. *J. Appl. Phys.* **1981**, *52*, 5934.
- (15) Lovinger, A. J. *Macromolecules* **1981**, *14*, 322.
- (16) Okada, K.; Watanabe, K.; Urushihara, T.; Toda, A.; Hikosaka, M. *Polymer* **2007**, *48*, 401.
- (17) Fillon, B.; Thierry, A.; Lotz, B.; Wittmann, J. C. *J. Therm. Anal.* **1994**, *42*, 721.
- (18) Ishida, H.; Bussi, P. *Macromolecules* **1991**, *24*, 3569.
- (19) Benkhathi, H.; Tan, T. T. M.; Jungnickel, B. *J. Polym. Sci., Part B: Polym. Phys.* **2001**, *39*, 2130.
- (20) Fillon, B.; Lotz, B.; Thierry, A.; Wittmann, J. C. *J. Polym. Sci., Part B: Polym. Phys.* **1993**, *31*, 1395.
- (21) Wittmann, J. C.; Lotz, B. *Prog. Polym. Sci.* **1990**, *15*, 909.
- (22) Qian, J.; Zhu, L.; Zhang, J.; Whitehouse, R. S. *J. Polym. Sci., Part B: Polym. Phys.* **2007**, *45*, 1564.
- (23) Kai, W.; Zhu, B.; Inoue, Y. *J. Polym. Sci., Part B: Polym. Phys.* **2005**, *43*, 2340.
- (24) Mead, W. T.; Zacharidas, A. E.; Shimada, T.; Porter, R. S. *Macromolecules* **1979**, *12*, 473.
- (25) Wunderlich, B. *Crystal Melting, Macromolecular Physics*, 3; Academic Press: New York, 1980.
- (26) Roberts, R. C. *Polymer* **1969**, *10*, 117.
- (27) Holdsworth, P. J.; Turner-Jones, A. *Polymer* **1971**, *12*, 195.
- (28) Kong, K.; Hay, J. N. *Polymer* **2003**, *44*, 623.
- (29) Morra, B. S.; Stein, R. S. *J. Polym. Sci., Part B: Polym. Phys.* **1982**, *20*, 2243.
- (30) Morra, B. S.; Stein, R. S. *J. Polym. Sci., Part B: Polym. Phys.* **1982**, *20*, 2261.
- (31) Braun, D.; Jacobs, M.; Hellmann, G. P. *Polymer* **1994**, *35*, 706.
- (32) Gregorio, R. *J. Appl. Polym. Sci.* **2006**, *100*, 3272.

MA702691C